

## Compound loss of GSDMD and GSDME function is necessary to achieve maximal therapeutic effect in colitis

Jianqiu Xiao<sup>a,1</sup>, Kai Sun<sup>a,1</sup>, Chun Wang<sup>a</sup>, Yousef Abu-Amer<sup>b,c</sup>, Gabriel Mbalaviele<sup>a,\*</sup>

<sup>a</sup> Division of Bone and Mineral Diseases, Washington University School of Medicine, St. Louis, MO, 63110, USA

<sup>b</sup> Department of Orthopaedic Surgery, Washington University School of Medicine, St. Louis, Missouri, USA

<sup>c</sup> Shriners Hospital for Children, St. Louis, Missouri, USA

### ARTICLE INFO

#### Keywords:

GSDMD  
GSDME  
DSS  
Colitis  
Inflammation  
Disulfiram

### ABSTRACT

Gasdermin D (GSDMD) and gasdermin E (GSDME) perpetuate inflammation by mediating the release of cytokines such as interleukin-1 $\beta$  (IL-1 $\beta$ ) and IL-18. However, not only are the actions of GSDMD in colitis still controversial, but its interplay with GSDME in the pathogenesis of this disease has not been investigated. We sought to fill these knowledge gaps using the dextran sodium sulfate (DSS) experimental mouse colitis model. DSS ingestion by wild-type mice caused body weight loss as the result of severe gut inflammation, outcomes that were significantly attenuated in *Gsdmd*<sup>-/-</sup> or *Gsdme*<sup>-/-</sup> mice and nearly fully prevented in *Gsdmd*<sup>-/-</sup>;*Gsdme*<sup>-/-</sup> animals. To assess the translational implications of these findings, we tested the efficacy of the active metabolite of US Food and Drug Administration (FDA)-approved disulfiram, which inhibits GSDMD and GSDME function. The severe DSS-induced gut toxicity was significantly decreased in mice treated with the inhibitor. Collectively, our findings indicate that disruption of the function of both GSDMD and GSDME is necessary to achieve maximal therapeutic effect in colitis.

### 1. Introduction

Genetic predispositions and environmental factors contribute to the pathogenesis of chronic inflammatory bowel disease (IBD), of which ulcerative colitis (UC) and Crohn disease (CD) are the most common manifestations [1,2]. UC mainly affects the mucosal lining of the colon and rectum whereas CD may affect any part of the gastrointestinal tract. These chronic relapsing-remitting disorders are associated with life-threatening complications, including considerable morbidity or risk of developing colorectal cancers [3,4]. Despite the encouraging data on clinical efficacy and mucosal healing, TNF- $\alpha$  antagonists are ineffective in up one-third of patients [5]. Thus, a better understanding of this disease is essential for developing efficacious and safe therapeutics.

The collapse of the gut epithelial barrier triggers unwanted interactions between the mucosal immune cells and colonic microflora

and subsequent inflammation in the gastrointestinal tract. IBD can be experimentally induced in animals by means of genetic manipulation (e.g., upon deletion of IL-10, TLR5, or T-bet) or upon exposure to chemicals (e.g., DSS, 2,4,6-trinitro-benzene sulfonic acid (TNBS), and oxazolone) [6–11]. Despite shortcomings such as the inability of each model to fully recapitulate the complexity of human conditions, these experimental models are amenable to mechanistic studies. For example, the DSS model provides insight into the contribution of innate immune networks in colitis pathogenesis, since the acute inflammatory response induced by this irritant is independent of T and B cells [12–14].

IBD pathogenesis is associated with dysregulated functions of inflammasomes, intracellular multiprotein complexes that are assembled by pathogen recognition receptors such as NLR family, pyrin domain containing 3 (NLRP3), absent in melanoma 2 (AIM2), or caspase-11 upon detection of microbial or sterile danger molecules

**Abbreviations:** AIM2,, absent in melanoma 2; ASC,, apoptosis-associated speck-like protein containing a CARD; CD,, Crohn disease; cGAS,, cyclic guanosine monophosphate-adenosine monophosphate (GMP-AMP) synthase; CuET,, bis(diethylthiocarbamate)-copper; DSS,, dextran sodium sulfate; GREM1,, gremlin 1; GSDMD,, gasdermin D; GSDME,, gasdermin E; IBD,, inflammatory bowel disease; IL-1 $\beta$ ,, interleukin-1 $\beta$ ; IL-1R1,, IL-1 receptor 1; NLRP3,, NLR family, CARD domain containing 3; NLRP3,, NLR family, pyrin domain containing 3; RSP03,, R-spondin 3; TNBS,, 2,4,6-trinitro-benzene sulfonic acid; UC,, ulcerative colitis.

\* Corresponding author. Division of Bone and Mineral Diseases, Washington University School of Medicine, 660 South Euclid Avenue, Campus Box 8301, St. Louis, MO, 63110.

E-mail address: [gmbalaviele@wustl.edu](mailto:gmbalaviele@wustl.edu) (G. Mbalaviele).

<sup>1</sup> These authors contributed equally to this work.

<https://doi.org/10.1016/j.jtauto.2022.100162>

Received 20 July 2022; Received in revised form 22 August 2022; Accepted 23 August 2022

Available online 30 August 2022

2589-9090/© 2022 Published by Elsevier B.V. This is an open access article under the CC BY-NC-ND license (<http://creativecommons.org/licenses/by-nc-nd/4.0/>).

[15–17]. Indeed, inactivation or inhibition of inflammasome component caspase-1 [18,19] or loss of NLRP3 [20] protects mice from DSS-induced colitis, and NLR family, CARD domain containing 4 (NLR4) gain-of-function mutations have been linked to autoinflammatory enterocolitis in humans [21]. These discoveries suggesting pathogenic actions of inflammasomes in colitis are conflicted by evidence indicating that NLRP3, AIM2, ASC, caspase-1, or caspase-11 deficient mice exhibit exacerbated DSS-induced colitis, though differences in disease severity are observed among these mouse strains [22–25]. Discrepant actions of the inflammasome products, IL-1 $\beta$  and IL-18, in IBD pathogenesis have also been reported. IL-1 or IL-18 signaling confers protection against DSS-induced colitis [23] as mice lacking *Il18*<sup>-/-</sup>, *Il18r1*<sup>-/-</sup>, or *Il1r*<sup>-/-</sup> display increased intestinal damage and histopathology [26,27]. Accordingly, a recent study reports that signaling downstream of IL-1 receptor 1 (IL-1R1) by R-spondin 3 (RSPO3) and IL-22 is important for epithelial recovery after *Citrobacter rodentium* infection whereas IL-1R1-dependent production of RSPO3 by gremlin 1 (GREM1)-positive mesenchymal cells alone is sufficient for recovery after DSS-induced colitis [28]. Yet, blockade of IL-18 or IL-1 signaling is claimed to alleviate DSS-induced colitis [3,20,29–31]. These conflicting results underscore the complexity of inflammasome actions in IBD pathogenesis.

Caspase-1 cleaves gasdermin D (GSDMD) [32,33], generating amino terminal fragments, which at the plasma membrane form IL-1 $\beta$  and IL-18 secretory conduits and can cause the lytic cell death pyroptosis [32–37]. High GSDMD levels in mucosal biopsies from patients with IBD suggest a pathogenic role for this protein in this disease; this observation is supported by the resistance of GSDMD deficient mice to DSS-induced gut inflammation [38] but is inconsistent with the severe colitis phenotype of another mouse strain lacking GSDMD [39]. In the latter report, GSDMD presumably preserves gut homeostasis by dampening cyclic guanosine monophosphate-adenosine monophosphate (GMP-AMP) synthase (cGAS) inflammatory actions in macrophages but not epithelial cells [39]. However, GSDMD can also promote caspase-8-dependent IL-1 $\beta$  secretion in intestinal epithelial cells (IECs) through pore formation-independent mechanisms involving the recruitment of Cdc37/Hsp90 and the E3 ligase, NEDD4, which catalyzes IL-1 $\beta$  poly-ubiquitination [38]. Evidence also implicates GSDME expressed by intestinal epithelial cells (IECs) in TNBS-induced colitis [40]. However, the interplay between GSDMD and GSDME during the pathogenesis of colitis has yet to be investigated.

To elucidate the role of GSDMD and GSDME in colitis, we administered DSS to mice with single or compound loss of these proteins or WT mice exposed to bis(diethylthiocarbamate)-copper (CuET), an inhibitor of GSDMD and GSDME [36]. We found that genetic inactivation of both GSDMD and GSDME was necessary to achieve maximal efficacy in the experimental colitis model. We also found that CuET was efficacious in this model. Since CuET is the active metabolite of disulfiram, a U.S. FDA-approved drug for the treatment of alcohol addiction, our findings lay ground for exploring the efficacy of this drug in IBD patients.

## 2. Materials and methods

### 2.1. Mice

*Gsdmd* knockout (*Gsdmd*<sup>-/-</sup>) mice were kindly provided by Dr. V.M. Dixit and Dr. N. Kayagki (Genentech, South San Francisco, CA). *Gsdme*<sup>-/-</sup> mice were purchased from Jackson Laboratory. All mice were on the C57BL6 background, and mouse genotyping was performed by PCR. All procedures were approved by the Institutional Animal Care and Use Committee (IACUC) of Washington University School of Medicine in St. Louis. All experiments were performed in accordance with the relevant guidelines and regulations described in the IACUC-approved protocol#19-0971.

### 2.2. DSS-induced colitis

For acute colitis induction, 2 month-old, number-, and sex-matched WT and littermate mutants were treated with 2.5% DSS (MP Bio-medicals, Ca# 216011025) in drinking water for 9 days. Body weights were recorded daily. Disease activity index (DAI) is the combined score of weight loss, stool consistency and body posture. The score was based on the following criteria: weight loss: 0 (no loss), 1 (5–10%), 2 (10–15%), 3 (>15%); stool consistency: 0 (normal), 1 (mild loose stool), 2 (loose stool), 3 (diarrhea and bloody stools); body posture: 0 (smooth fur without a hunchback), 1 (mild fur and hunchback), 2 (moderate fur and hunchback), 3 (severe fur and hunchback). At the indicated time points, mice were euthanized and colons were collected for length measurements, explant cultures, immunoblotting, and histology.

### 2.3. CuET administration

CuET (TCI America, OR) was prepared in DMSO. Mice were intraperitoneally injected with vehicle or 1 mg/kg CuET, once every other day. Samples were harvested 48 h after the last CuET injection (Fig. 3A).

### 2.4. Colon explant culture

Colons were collected from mice, washed for three times in cold PBS containing gentamicin (20  $\mu$ g/ml), penicillin G (200  $\mu$ g/ml) and streptomycin (200  $\mu$ g/ml), cut into pieces, and cultured for 24 h at 37 °C in DMEM supplemented with 10% FBS. The conditioned media were collected for ELISA.

### 2.5. Histology

Harvested colons were fixed in 10% neutral buffered formalin for 16–24 h, embedded in paraffin, and sectioned at 5  $\mu$ m thickness. The sections were stained with hematoxylin-eosin (HE) and blindly scored for intestinal architecture damage (scores from 0 to 4) and inflammatory cell infiltrates (scores from 0 to 4). Photographs were taken using ZEISS microscopy (Carl Zeiss Industrial Metrology, MN).

### 2.6. Western blot

Harvested colons were lysed with RIPA buffer (50 mM Tris, 150 mM NaCl, 1 mM EDTA, 0.5% NaDOAc, 0.1% SDS, and 1.0% NP-40) plus Complete Protease Inhibitor Cocktail and phosphatase inhibitors (Roche). Protein concentrations of tissue lysates were determined by Bio-Rad method. Proteins were separated by SDS-PAGE (12%) and transferred to PVDF membrane. Proteins were stained as previously described [36,41,42]. Briefly, the membranes were incubated with antibodies against GSDMD (1:1000, ab209845, Abcam), GSDME (1:1000, ab215191, Abcam), IL-1 $\beta$  (1:2500, ab9722, Abcam), or  $\beta$ -actin (1:5000, sc-47778, Santa Cruz Biotechnology) overnight at 4 °C, followed by a 1 h incubation with secondary goat anti-rabbit IgG (1:5000, A21109, Thermo Fisher Scientific) or goat anti-mouse IgG (1:5000, A21058, Thermo Fisher Scientific), respectively. The results were developed using Li-Cor Odyssey Infrared Imaging System (LI-COR Biosciences).

### 2.7. ELISA for IL-18 and IL-1 $\beta$

IL-1 $\beta$  and IL-18 levels were measured using the eBioscience ELISA kits (eBiosciences, Grand Island, NY; RAB0810, Sigma-Aldrich, MO, respectively).

### 2.8. Statistical analysis

Statistical analysis was performed using one-way ANOVA with Tukey's multiple comparisons test or two-way ANOVA with Tukey's multiple comparisons test in GraphPad Prism7.

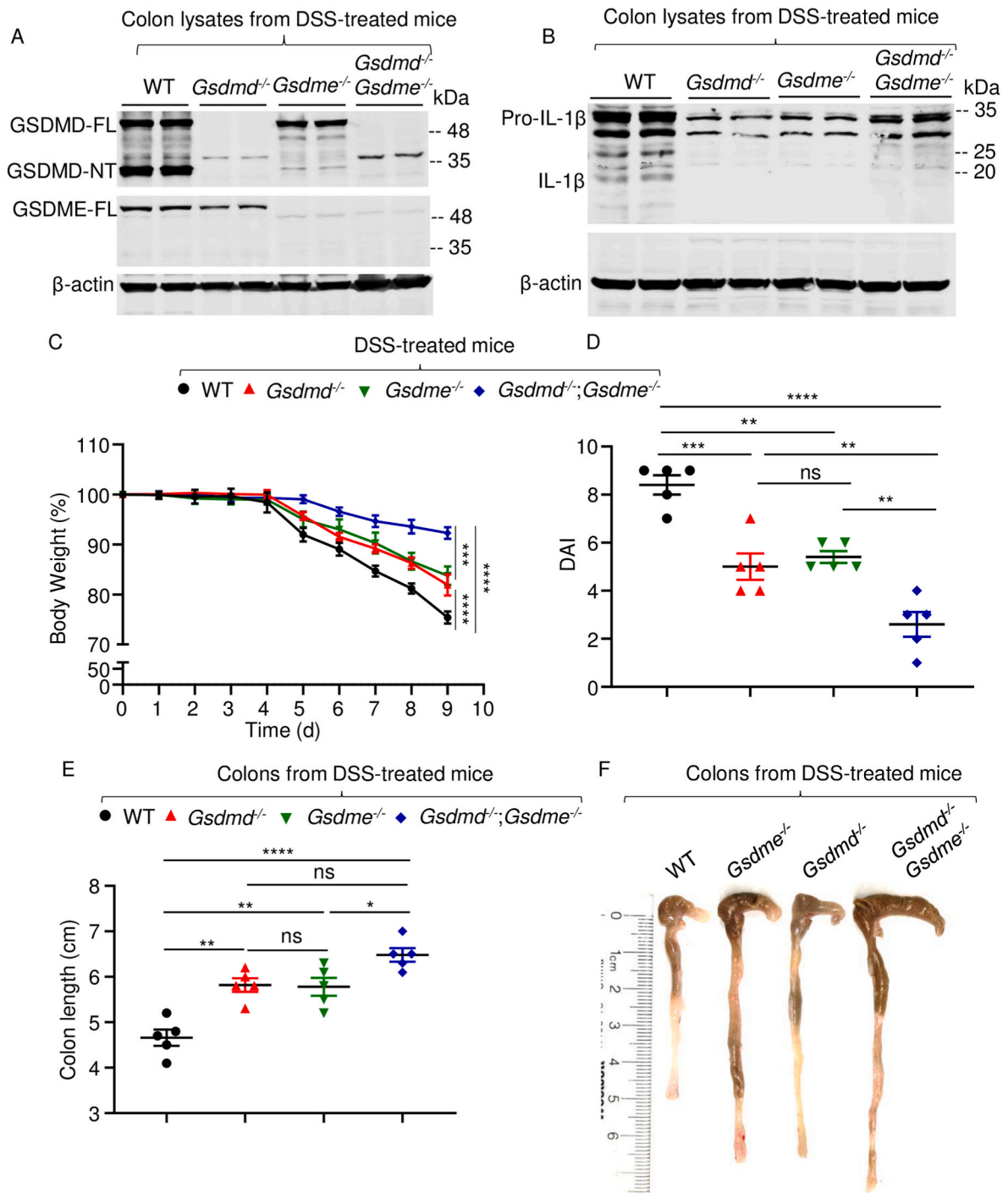


**Fig. 1. Loss of GSDMD or GSDME attenuated DSS-induced colitis.** Mice were administrated with 2.5% DSS in drink water for 9 days. (A and B) Colon lysates were analyzed by immunoblotting. (C) Mouse body weight, recorded daily. (D) DAI. (E) Colon length. (F) Representative images of the colons. Data are mean ± SEM. N = 5 mice/group. \**p* < 0.05; \*\**p* < 0.005; \*\*\**p* < 0.0005; \*\*\*\**p* < 0.0001. One-Way ANOVA or Two-Way ANOVA. DAI, disease activity index; FL, full-length; ns, non-significant; WT, wild-type.

### 3. Results

#### 3.1. Inactivation of *Gsdmd* or *Gsdme* attenuated DSS-induced colitis

Proteolytic cleavage of GSDMD and GSDME generates amino-terminal fragments (GSDMD-NT and GSDME-NT, respectively), which are endowed with pore-forming activity [32–37]. To determine the fate of GSDMD and GSDME in colitis-associated acute inflammation, we fed mice with DSS polymers in the drinking water and analyzed the

processing of these proteins in colon lysates. Immunoblotting analysis revealed that GSDMD full-length (GSDMD-FL) and GSDME-FL were readily detected in samples from wild-type (WT) but not the corresponding null mice, as expected (Fig. 1A). Loss of GSDMD resulted in slightly decreased GSDME-FL levels, and vice-versa. Unlike GSDME-NT, GSDMD-NT was readily detected in samples from DSS-treated WT mice, and barely in samples from *Gsdme* knockout (*Gsdme*<sup>-/-</sup>) mice treated with this irritant (Fig. 1A). Pro-IL-1β levels were markedly decreased in samples from knockout mice compared to WT counterparts (Fig. 1B). As

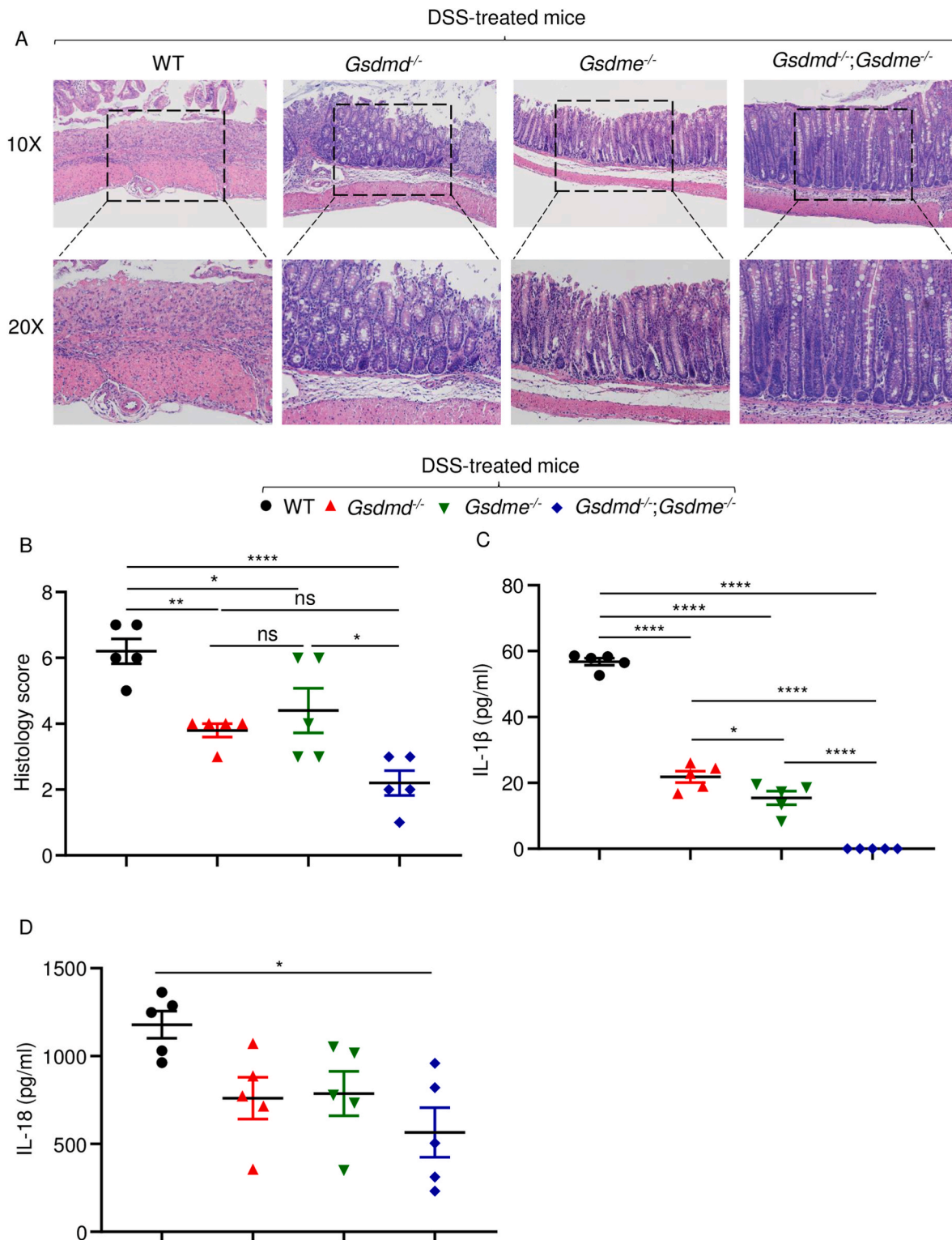


**Fig. 2.** Loss of GSDMD or GSDME attenuated DSS-induced colon damage and cytokine secretion. Mice were administrated with 2.5% DSS in drink water for 9 days. Colons were collected for histology or tissue culture. (A) Representative of histology pictures for each mouse. (B) Histology score for each mouse group. (C) IL-1β concentrations in tissue culture medium. (D) IL-18 concentrations in tissue culture medium. Data are mean ± SEM. N = 5 mice/group. \**p* < 0.05; \*\**p* < 0.005; \*\*\*\**p* < 0.0001. One-Way ANOVA. NS, non-significant; WT, wild-type.

a result, mature IL-1β p17 was detected only in WT samples (Fig. 1B). Thus, the maturation of GSDMD and IL-1β, but not GSDME, is readily noticeable in the colon lysates from DSS-treated WT mice.

To determine the impact of GSDMD and/or GSDME deficiency on DSS-induced colitis, we assessed a battery of reliable surrogate marker of

morbidity associated with this disease in WT and mutant mice. Oral administration of the sulfated polysaccharide DSS to WT mice caused body weight loss noticeable by day 5, reaching up to 25% by day 9 post-treatment (Fig. 1C). DSS-exposed *Gsdmd*<sup>-/-</sup> and *Gsdme*<sup>-/-</sup> mice also lost body weight equally but to a significantly lesser extent compared to WT



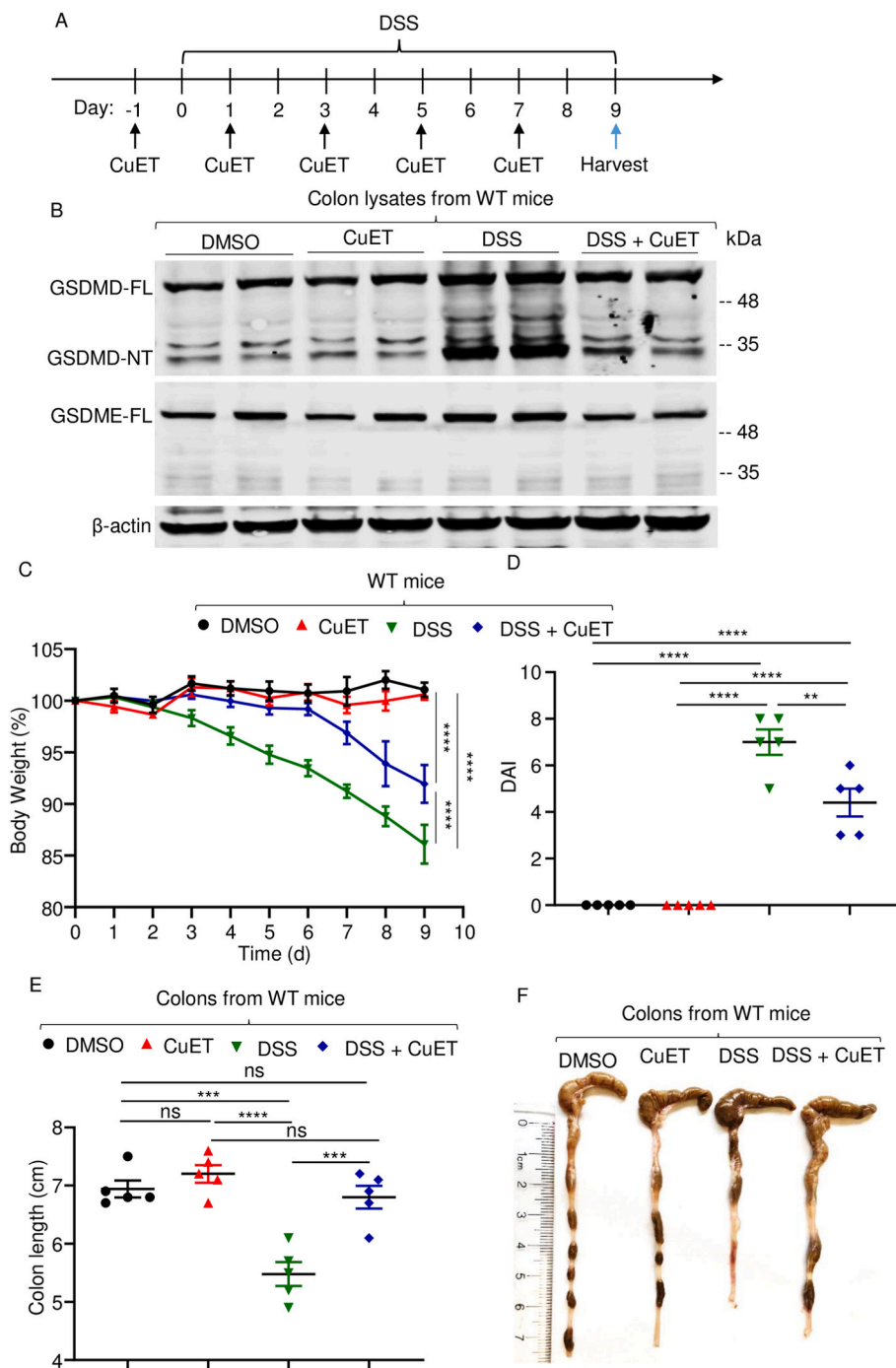


**Fig. 3. CuET attenuated DSS-induced colitis.** Mice were pre-treated with vehicle or 1 mg/kg CuET one day prior to exposure to vehicle or 2.5% DSS in drink water. (A) Experimental design. (B) Colon lysates were analyzed by immunoblotting. (C) Mouse body weight, recorded daily. (D) DAI. (E) Colon length. (F) Representative images of the colons. Data are mean  $\pm$  SEM. N = 5 mice/group.  $^{**}p < 0.005$ ;  $^{***}p < 0.0005$ ;  $^{****}p < 0.0001$ . One-Way ANOVA or Two-Way ANOVA. CuET, bis(diethylthiocarbamate)-copper; DAI, disease activity index; FL, full-length; ns, non-significant; WT, wild-type.

cohorts (Fig. 1C). Remarkably, compound knockout mice barely lost body weight during the evaluation period of this study (Fig. 1C). Accordingly, disease activity index (DAI) score, which was similarly lower in *Gsdmd*<sup>-/-</sup> and *Gsdme*<sup>-/-</sup> mice compared to WT littermates was further decreased in *Gsdmd*<sup>-/-</sup>;*Gsdme*<sup>-/-</sup> mice (Fig. 1D). We also measured colon length, the parameter with the lowest variability in the model of DSS-induced colitis [14]. The colons were longer in *Gsdmd*<sup>-/-</sup> and *Gsdme*<sup>-/-</sup> mice compared to WT controls, but shorter relative to *Gsdmd*<sup>-/-</sup>;*Gsdme*<sup>-/-</sup> mice (Fig. 1E and F).

Histopathological analysis of hematoxylin and eosin (H&E)-stained colonic sections from DSS-treated WT mice showed severely compromised integrity of the mucosal barrier, loss of epithelial cells, and massive neutrophil infiltrations (Fig. 2A and B). These outcomes were significantly attenuated in *Gsdmd*<sup>-/-</sup> or *Gsdme*<sup>-/-</sup> mice, though to a

lesser extent in the latter cohort. Remarkably, double knockout mice appeared protected from DSS-induced tissue damage (Fig. 2A and B). Consistent with histopathological findings, IL-1 $\beta$  and IL-18 levels were lower in cultured colon explants from *Gsdmd*<sup>-/-</sup> and *Gsdme*<sup>-/-</sup> mice compared to WT controls, but further decreased or undetectable in those from *Gsdmd*<sup>-/-</sup>;*Gsdme*<sup>-/-</sup> mice (Fig. 2C and D). Collectively, these results suggest that GSDMD and GSDME play an important role in DSS-induced inflammation in the colon and the ensuing tissue damage.

### 3.2. CuET inhibited DSS-induced colitis

Since GSDMD and GSDME are implicated in colitis [38–40], recent data indicating that CuET inhibits the maturation and pore-forming activity of these proteins provided a strong rationale for translational

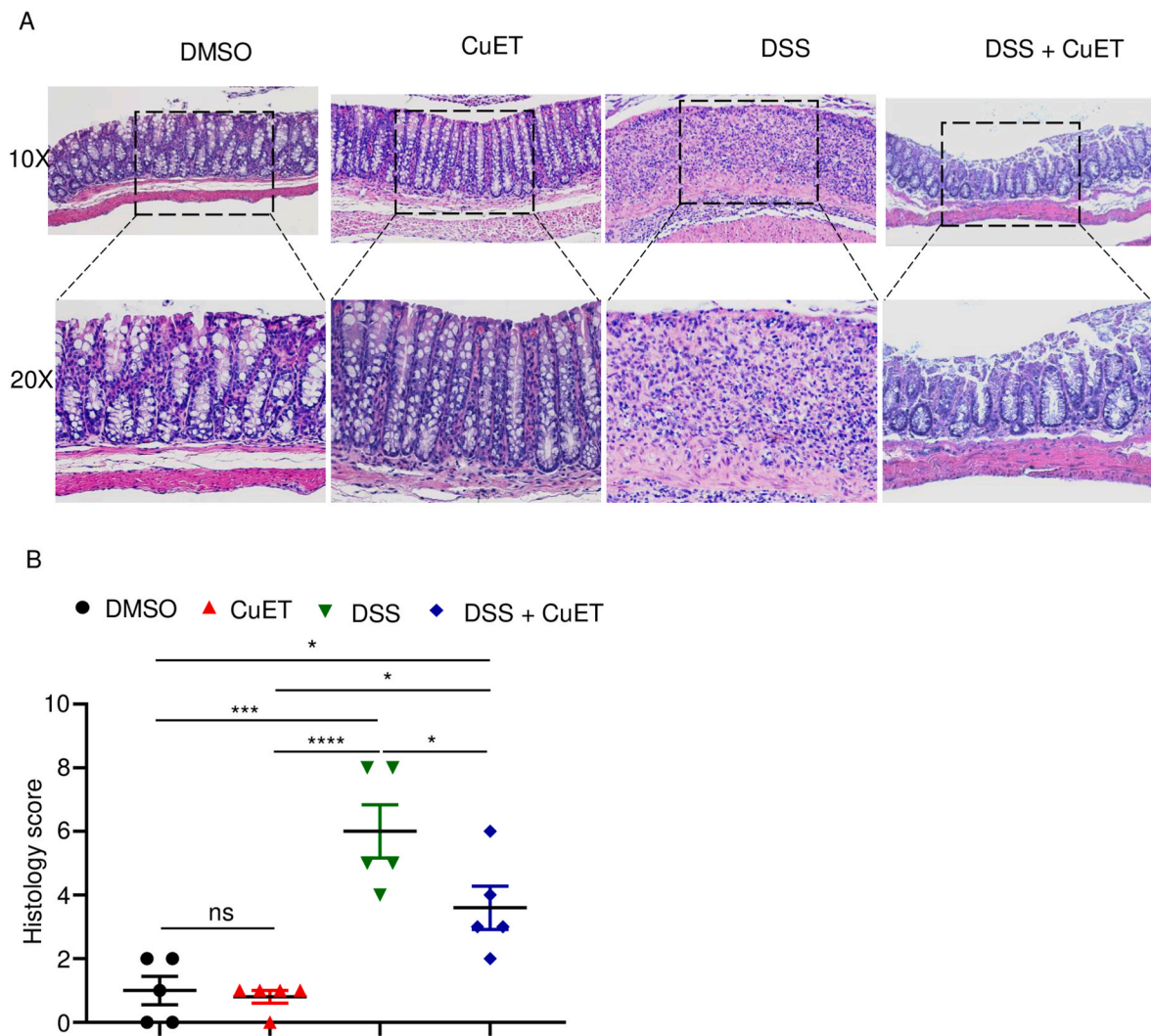


**Fig. 4. CuET attenuated DSS-induced colon damage.** Mice were pre-treated with 1 mg/kg CuET one day prior to exposure to 2.5% DSS in drink water. (A) Representative of histology pictures for each mouse. (B) Histology score for each group of mice. Data are mean ± SEM. N = 5 mice/group. \**p* < 0.05; \*\*\**p* < 0.0005; \*\*\*\**p* < 0.0001. One-Way ANOVA. CuET, bis(diethyldithiocarbamate)-copper; ns, non-significant; WT, wild-type.

studies aimed at testing the efficacy of this drug in colitis, as outlined in Fig. 3A. Immunoblotting analysis revealed that CuET administration did not affect baseline GSDMD and GSDMD-NT levels in colon lysates from naïve WT mice (Fig. 3B). DSS treatment increased the levels of GSDMD-FL and GSDMD-NT, but failed to induce this response in mice pre-treated with CuET (Fig. 3B). Likewise, GSDME-FL steady-state levels were unaffected by CuET. DSS slightly increased GSDME-FL levels, but GSDME-NT was not detected in any of these conditions (Fig. 3B), findings that are consistent with those shown in Fig. 1A.

Consistent with the result described above (Fig. 1C), administration of DSS to WT mice caused time-dependent body weight loss starting on day 2 and progressing linearly until day 9 post-treatment (Fig. 3C). CuET did not affect body weight of naïve mice throughout the duration of this study, suggesting that it was well tolerated. Importantly, treatment with CuET delayed DSS-induced body weight as it was not different from untreated mice until day 6 post-treatment (Fig. 3C). CuET also attenuated DAI score (Fig. 3D) and disease-associated colon shortening (Fig. 3E and F) compared to WT controls. H&E-based histopathological analysis revealed that colonic architecture of naïve mice was unperturbed by CuET treatment (Fig. 4A). DSS-induced toxicity, which included epithelial defects, crypt atrophy, and massive neutrophil infiltrations, was reduced in CuET-treated mice (Fig. 4A and B). Thus, the severe gut pathology caused by DSS in mice is attenuated upon treatment with

CuET.

#### 4. Discussion

We found that amino-terminal pore-forming fragments from GSDMD but not GSDME were readily detected in colon extracts from mice exposed to DSS. Our inability to detect GSDME-NT fragments in DSS-treated mice was unexpected given the comparable colitogenic phenotype of mice lacking GSDMD or GSDME. Although secretory conduits assembled by amino-terminal fragments and ultimately cell lysis are the main mechanism of GSDM actions, a recent study reported the lytic activity-independent function of GSDMD in colitis [38]. Therefore, it is tempting to speculate that GSDME may promote colitis independently of its processing and pore-forming activity. Alternatively, GSDME amino-terminal fragments may have been undetectable simply because they were lost from pyroptotic cells as immunoblotting analyses were carried out using sample extracts from mainly non-pyroptotic cell lysates. Our results underscore the complexity of evaluating GSDME fate *in vivo*. This view is supported by a recent report indicating that cleaved GSDMD fragments were readily detected in myeloid cells but barely in IECs of mice exposed to DSS even with comparable expression levels of GSDMD in both cell compartments [39]. Despite apparent differences in the fate of these GSDMs, as noted above, we found that inactivation of

*Gsdmd* or *Gsdme* attenuates DSS-induced colitis, an outcome further reduced in double knockout mice. These results are consistent with recent reports indicating that GSDMD or GSDME deficiency reduced the severity of experimental colitis [38,40], but they conflict with others' findings implicating GSDMD in the pathogenesis of colitis [39]. Biological variables that underlie these discrepancies are unclear but may include the age, sex, strains, and microbiota composition of mice.

We discovered that CuET inhibits DSS-induced colitis, an outcome that correlated with inhibition of GSDMD cleavage and decreased levels of GSDME-FL. Residual inflammatory responses in CuET-treated mice may be due to suboptimal dosing regimens, as serum concentrations of the drug were not monitored to ensure that appropriate exposure levels were achieved. CuET inactivates GSDMD presumably by modifying Cys191, but the mechanisms of its inhibition of GSDME remain unclear. Despite shortcomings in the mechanisms of action of CuET, the results reported here are consistent with its efficacy in autoimmune and auto-inflammatory disease models [36,43,44].

Our findings demonstrate that genetic inactivation of GSDMD and GSDME or functional blockade of these proteins by CuET inhibits the pathogenesis of experimental colitis. They provide a rationale for evaluating the utility of this drug for the treatment of IBD in human patients.

### Data availability

This study includes no data deposited in external repositories.

### Author contributions

Study conception and design: JX, GM. Acquisition of data and methodology: JX, KS, CW. Analysis and interpretation of data: JX, KS, CW, YA, GM. <sup>#</sup>Editing: JX, YA. Writing: JX, GM.

### Declaration of competing interest

Dr. Gabriel Mbalaviele is consultant for Aclaris Therapeutics, Inc. All other authors declare no conflict of interest.

### Acknowledgments

This work was supported by NIH/NIAMS AR076758 and AI1161022 grants to GM; YA-A by NIH grants AR049192, AR074992, AR072623, and by grant #85160 from the Shriners Hospital for Children.

We thank Dr. Deborah J. Veis and Dustin Kress for reading the manuscript.

### References

- [1] G. Wark, et al., The role of diet in the pathogenesis and management of inflammatory bowel disease: a review, *Nutrients* 13 (1) (2020).
- [2] S. Danese, M. Sans, C. Fiocchi, Inflammatory bowel disease: the role of environmental factors, *Autoimmun. Rev.* 3 (5) (2004) 394–400.
- [3] V. Neudecker, et al., Myeloid-derived miR-223 regulates intestinal inflammation via repression of the NLRP3 inflammasome, *J. Exp. Med.* 214 (6) (2017) 1737–1752.
- [4] M.C. Fantini, I. Guadagni, From inflammation to colitis-associated colorectal cancer in inflammatory bowel disease: pathogenesis and impact of current therapies, *Dig. Liver Dis.* 53 (5) (2021) 558–565.
- [5] E. Troncone, et al., Novel therapeutic options for people with ulcerative colitis: an update on recent developments with janus kinase (JAK) inhibitors, *Clin. Exp. Gastroenterol.* 13 (2020) 131–139.
- [6] J. Miyoshi, et al., Early-life microbial restitution reduces colitis risk promoted by antibiotic-induced gut dysbiosis in interleukin 10(-/-) mice, *Gastroenterology* 161 (3) (2021) 940–952 e15.
- [7] W. Strober, I.J. Fuss, Proinflammatory cytokines in the pathogenesis of inflammatory bowel diseases, *Gastroenterology* 140 (6) (2011) 1756–1767.
- [8] S. Wirtz, et al., Chemically induced mouse models of acute and chronic intestinal inflammation, *Nat. Protoc.* 12 (7) (2017) 1295–1309.
- [9] S. Wirtz, et al., Chemically induced mouse models of intestinal inflammation, *Nat. Protoc.* 2 (3) (2007) 541–546.
- [10] V. Singh, et al., Proneness of TLR5 deficient mice to develop colitis is microbiota dependent, *Gut Microb.* 6 (4) (2015) 279–283.
- [11] K.H. Jung, et al., Intratracheal ovalbumin administration induces colitis through the IFN-gamma pathway in mice, *Front. Immunol.* 10 (2019) 530.
- [12] K. Ke, et al., Attenuation of NF-kappaB in intestinal epithelial cells is sufficient to mitigate the bone loss comorbidity of experimental mouse colitis, *J. Bone Miner. Res.* 34 (10) (2019) 1880–1893.
- [13] B. Chassaing, et al., Dextran sulfate sodium (DSS)-induced colitis in mice, *Curr. Protoc. Im.* 104 (2014) 15 25 1–15 25 14.
- [14] I. Okayasu, et al., A novel method in the induction of reliable experimental acute and chronic ulcerative colitis in mice, *Gastroenterology* 98 (3) (1990) 694–702.
- [15] V.A.K. Rathinam, F.K. Chan, Inflammasome, inflammation, and tissue homeostasis, *Trends Mol. Med.* 24 (3) (2018) 304–318.
- [16] A. Pandey, C. Shen, S.M. Man, Inflammasomes in colitis and colorectal cancer: mechanism of action and therapies, *Yale J. Biol. Med.* 92 (3) (2019) 481–498.
- [17] V. Khatri, R. Kalyanasundaram, Therapeutic implications of inflammasome in inflammatory bowel disease, *Faseb. J.* 35 (5) (2021), e21439.
- [18] B. Siegmund, et al., IL-1 beta -converting enzyme (caspase-1) in intestinal inflammation, *Proc. Natl. Acad. Sci. U. S. A.* 98 (23) (2001) 13249–13254.
- [19] C. Bauer, et al., The ICE inhibitor pralnacasan prevents DSS-induced colitis in C57BL/6 mice and suppresses IP-10 mRNA but not TNF-alpha mRNA expression, *Dig. Dis. Sci.* 52 (7) (2007) 1642–1652.
- [20] C. Bauer, et al., Colitis induced in mice with dextran sulfate sodium (DSS) is mediated by the NLRP3 inflammasome, *Gut* 59 (9) (2010) 1192–1199.
- [21] N. Romberg, et al., Mutation of NLRC4 causes a syndrome of enterocolitis and autoinflammation, *Nat. Genet.* 46 (10) (2014) 1135–1139.
- [22] I.C. Allen, et al., The NLRP3 inflammasome functions as a negative regulator of tumorigenesis during colitis-associated cancer, *J. Exp. Med.* 207 (5) (2010) 1045–1056.
- [23] M.H. Zaki, et al., The NLRP3 inflammasome protects against loss of epithelial integrity and mortality during experimental colitis, *Immunity* 32 (3) (2010) 379–391.
- [24] R.A. Ratsimandresy, et al., The AIM2 inflammasome is a central regulator of intestinal homeostasis through the IL-18/IL-22/STAT3 pathway, *Cell. Mol. Immunol.* 14 (1) (2017) 127–142.
- [25] D. Demon, et al., Caspase-11 is expressed in the colonic mucosa and protects against dextran sodium sulfate-induced colitis, *Mucosal Immunol.* 7 (6) (2014) 1480–1491.
- [26] H. Takagi, et al., Contrasting action of IL-12 and IL-18 in the development of dextran sodium sulphate colitis in mice, *Scand. J. Gastroenterol.* 38 (8) (2003) 837–844.
- [27] S.L. Lebeis, et al., Interleukin-1 receptor signaling protects mice from lethal intestinal damage caused by the attaching and effacing pathogen *Citrobacter rodentium*, *Infect. Immun.* 77 (2) (2009) 604–614.
- [28] C.B. Cox, et al., IL-1R1-dependent signaling coordinates epithelial regeneration in response to intestinal damage, *Sci. Immunol.* 6 (59) (2021).
- [29] P.V. Sivakumar, et al., Interleukin 18 is a primary mediator of the inflammation associated with dextran sulphate sodium induced colitis: blocking interleukin 18 attenuates intestinal damage, *Gut* 50 (6) (2002) 812–820.
- [30] B. Siegmund, et al., Neutralization of interleukin-18 reduces severity in murine colitis and intestinal IFN-gamma and TNF-alpha production, *Am. J. Physiol. Regul. Integr. Comp. Physiol.* 281 (4) (2001) R1264–R1273.
- [31] S.U. Seo, et al., Distinct commensals induce interleukin-1beta via NLRP3 inflammasome in inflammatory monocytes to promote intestinal inflammation in response to injury, *Immunity* 42 (4) (2015) 744–755.
- [32] N. Kayagaki, et al., Caspase-11 cleaves gasdermin D for non-canonical inflammasome signalling, *Nature* 526 (7575) (2015) 666–671.
- [33] J. Shi, et al., Cleavage of GSDMD by inflammatory caspases determines pyroptotic cell death, *Nature* 526 (7575) (2015) 660–665.
- [34] Z. Zhang, et al., Gasdermin E suppresses tumour growth by activating anti-tumour immunity, *Nature* 579 (7799) (2020) 415–420.
- [35] J. Ding, et al., Pore-forming activity and structural autoinhibition of the gasdermin family, *Nature* 535 (7610) (2016) 111–116.
- [36] C. Wang, et al., NLRP3 inflammasome activation triggers gasdermin D-independent inflammation, *Sci. Immunol.* 6 (64) (2021) eabj3859.
- [37] C. Rogers, et al., Cleavage of DFNA5 by caspase-3 during apoptosis mediates progression to secondary necrotic/pyroptotic cell death, *Nat. Commun.* 8 (2017), 14128.
- [38] K. Bulek, et al., Epithelial-derived gasdermin D mediates nonlytic IL-1beta release during experimental colitis, *J. Clin. Invest.* 130 (8) (2020) 4218–4234.
- [39] C. Ma, et al., Gasdermin D in macrophages restrains colitis by controlling cGAS-mediated inflammation, *Sci. Adv.* 6 (21) (2020) eaaz6717.
- [40] G. Tan, et al., Gasdermin-E-mediated pyroptosis participates in the pathogenesis of Crohn's disease by promoting intestinal inflammation, *Cell Rep.* 35 (11) (2021), 109265.
- [41] J. Xiao, et al., Gasdermin D mediates the pathogenesis of neonatal-onset multisystem inflammatory disease in mice, *PLoS Biol.* 16 (11) (2018) e3000047.
- [42] J. Xiao, et al., Radiation causes tissue damage by dysregulating inflammasome-gasdermin D signaling in both host and transplanted cells, *PLoS Biol.* 18 (8) (2020) e3000807.
- [43] J.J. Hu, et al., FDA-approved disulfiram inhibits pyroptosis by blocking gasdermin D pore formation, *Nat. Immunol.* 21 (7) (2020) 736–745.
- [44] X. Huang, et al., Disulfiram attenuates MCMV-Induced pneumonia by inhibition of NF-kappaB/NLRP3 signaling pathway in immunocompromised mice, *Int. Immunopharm.* 103 (2022), 108453.